

DEFORMATION BEHAVIOR OF REINFORCED CONCRETE BEAMS DETERIORATED BY ASR

W. KOYANAGI, K. ROKUGO, Y. UCHIDA & H. IWASE
Department of Civil Engineering, Gifu University,
(1-1 Yanagido, Gifu-city, JAPAN)

ABSTRACT

Experimental studies were made on the behavior of singly reinforced concrete beams without shear reinforcement which were severely deteriorated with wide cracks caused by alkali-silica reaction (ASR). Analytical study was also made on the mechanical property of the beams, especially on the effect of pre-stress caused by the restriction of ASR expansion by reinforcement. Compared with beams without deterioration, yield starting bending moment of the severely deteriorated beams decreased. There are two possible reasons. One is because neutral axis depth increased and the length of moment arm decreased due to the presence of prestress, and the other is low Young's modulus. In case of the deteriorated beams, deflections at the yield starting point decreased because flexural rigidity of the deteriorated beams increased. The ultimate bending moment did not change, whether deterioration due to ASR was heavy or nil, because after the start of yielding, flexural cracks extended and moment arm length increased rapidly even in case of the deteriorated beams and the length, consequently the ultimate moment, came to be the same.

Keywords: ASR, beam, deformation, yield starting moment, ultimate bending moment

INTRODUCTION

Various approaches have been made to investigate the mechanical properties of reinforced concrete members damaged by alkali-silica reaction (ASR) for the safety assessment of damaged structures.

It has been reported, as a result of loading tests on beam members, that the stress due to ASR-induced expansion restrained by reinforcement increases the rigidity of the member, in some cases shifting the failure mode from shear to flexure (Hobbs 1988) and enhances shear capacity (Cope & Slade 1992). ASR damage therefore does not necessarily reduce the ultimate load-bearing capacity, but rather can increase it (Koyanagi *et al.* 1987). While, it has also been reported that such damage reduces the yield strength of beams (Inoue *et al.* 1989), and this has been ascribed to the effects of the existing stress of reinforcement.

The authors discuss here the mechanical properties of reinforced concrete beams with different steel ratio, which were deteriorated severely by ASR with crack widths of 0.6 to 0.7 mm. Static loading tests were made on the reinforced concrete beam specimens with and without deterioration, and strength properties such as cracking, yield and ultimate moments as well as deformation properties were obtained. Analytical study was also made especially on deformation properties.

EXPERIMENTAL PROCEDURE

Scope of the experiments

The beam specimens investigated were rectangular beams 10x18x170 cm in size with singly reinforcement and without shear reinforcement. Two levels of

reinforcement ratios, "S" and "L", were employed as variables in combination with Series A with ASR damage due to alkali addition and Series N with no ASR damage. These made four types of beam specimens: AS, NS, AL, and NL beams.

Materials and mix proportions

The cement used was ordinary portland cement (Equivalent $\text{Na}_2\text{O} = 0.61\%$). As for the fine aggregate, non-reactive sand from the Nagara River was used. As for coarse aggregates, gravel from the Nagara River and crushed bronzite andesite (Dissolved silica:Sc = 180, Reduction in alkalinity:Rc = 124 mmol/lit) were used as inert and reactive coarse aggregates, respectively. As reinforcement, deformed bars of 10mm (D10: $f_y = 380$ MPa, $f_u = 535$ MPa) and of 13 mm (D13: $f_y = 371$ MPa, $f_u = 556$ MPa) were used.

The unit content of water and cement was 176 and 352 kg/m^3 , respectively. The sand-aggregate ratio was 0.45. When using the reactive aggregate, its portion was adjusted to 60% of the total coarse aggregate. The alkali to be added is Na_2SO_3 , which has a high reactivity while scarcely affecting the concrete properties. Total equivalent Na_2O content of 3% of cement weight was adopted. The slump and air content of freshly mixed concrete were approximately 10 cm and 4%, respectively, for both N and A specimens.

Specimen, loading and measurement

The beam specimens were fabricated using two D10 or D13 bars as the main reinforcement with a cover depth of 20 mm. The steel ratios of S and L specimens were 0.92% and 1.66%, respectively. Shear reinforcement was not provided.

The beam specimens were wet-cloth-cured in a thermostatic chamber of 20°C for 4 weeks after demolding. "A" beams were then spray-cured with the room temperature raised to 40°C for approximately 4 months to accelerate ASR, and then left in the thermostatic chamber of 20°C. "N" beams were left in a laboratory atmosphere for 4 weeks after being wet-cloth-cured.

Loading tests were conducted on the beam specimens at an age of 2 years. The loading was applied on two symmetrical points with a span of 125 cm. Two A beams and one N beam of Series S and Series L were tested. The following measurements were made: the loads, the displacements at the loading points and supporting points and the longitudinal deformations on one side of the beam within the moment span by high-sensitivity displacement gages fixed at 3 cm from the top and bottom, with the gage length of 20 cm. The state of the loading and measuring manner and the cross section of the specimen are shown in Fig. 1.

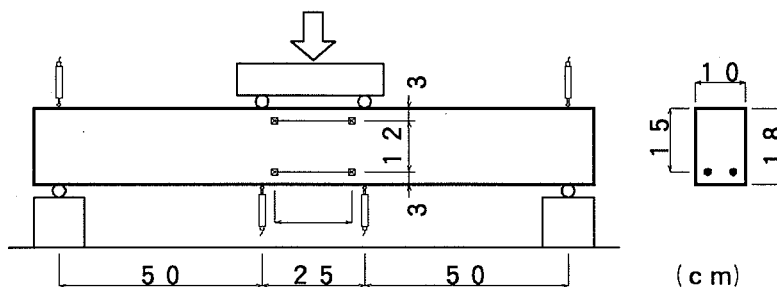


Fig. 1. Loading and measuring manner and cross section of beam.

Along with the beam tests, various mechanical properties of concrete were obtained; the static Young's modulus and compressive strength using specimens 10 cm in diameter and 20 cm in length, the dynamic Young's modulus and flexural strength using specimens 10 x 10 x 40 cm in size, and the splitting tensile strength using specimens 15 cm in diameter and 15 cm in length. These specimens were cured and stored as same manner as beam specimens.

RESULTS OF EXPERIMENT

Cracking due to ASR

Numerous cracks developed in A beams during the spray curing at 40°C. The cracks concentrated mostly in the upper part of the beams where no reinforcement was provided. The cracks were mostly longitudinal near the vertical center and transverse on the top edge, and the width of some of them reached 0.6 to 0.7 mm. Typical crack patterns are shown in Fig. 2. Both S and L beams showed a warp (upward deflection) of 12 to 14 mm for total length of 140 cm. The differences in the reinforcement ratio led to no significant differences in the cracking pattern and the amount of warp.

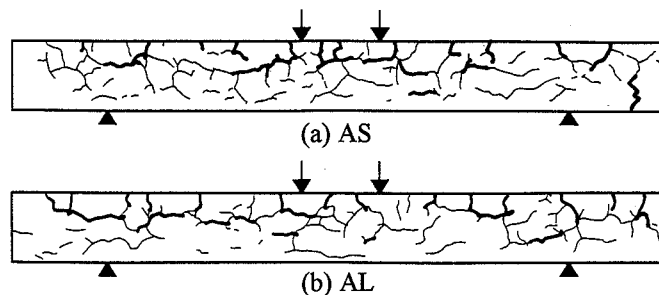


Fig. 2. Typical crack pattern of deteriorated beams

Results of beam test

All the S series beams failed in flexure. On the other hand, in the L series with a large reinforcement ratio, the N beams without ASR showed a shear failure, while the A beams with ASR showed a flexural failure.

The initial portion and the whole measured load-displacement curves of the beams are shown in Figs. 3a and 3b, respectively. The curves of the A beam couples agree well for both S and L. From Fig. 3a, both S and L beams of Series A have higher initial rigidity than those of Series N. The load at which the slope of the curves abruptly changes, which corresponds to the first crack, is 60% or more higher for Series A than for Series N. Fig. 3b reveals that, regarding the S beams, which failed in flexure, the yield starting point of Series A is approximately 10% lower than that of Series N, but the load-carrying capacity of Series A increases as the deformation increases after yielding, resulting in almost the same or slightly larger ultimate load-bearing capacity than that of Series N. The maximum loading point can be called as the strength failure point. The deformation at the strength failure point of series A is larger than that of series N. As for the L beams, a direct comparison is difficult, because the Series N beam failed in shear. However, a marked increase is observed in the load-bearing capacity of

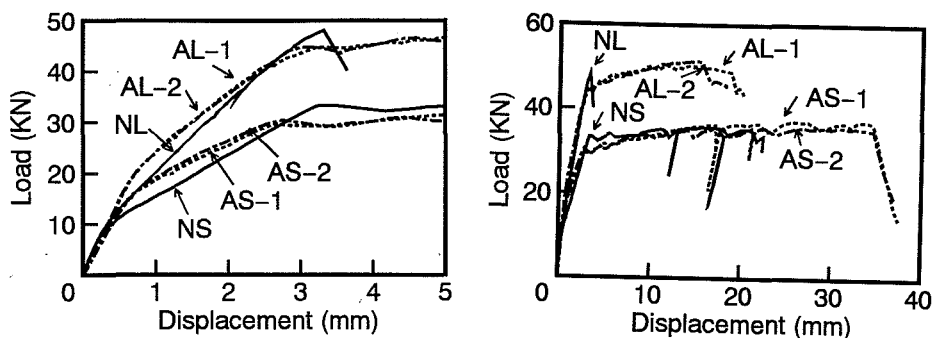


Fig. 3. Load-displacement curve (left:initial part, right:entire part)

Series A associated with the deformation after yield starting, similarly to the case of the S beams. Series A had a 6% higher ultimate load-bearing capacity and sufficiently larger deformation at the strength failure point than that of Series N, because shear failure occurred in Series N. Measured cracking moment (M_c), yield starting moment (M_y), and the maximum moment (M_u) of the beams are tabulated in Table 1. The depth of the neutral axis was calculated from the measured strains. The changes in the neutral axis depth are shown in Fig. 4 with the neutral axis ratio η which is defined as the ratio of the depth of neutral axis to its effective depth. The neutral axis ratios decreased gradually when applied load increased. The ratio decreased rapidly after yield starting the bars. The ratio of Series A at the time of the yield starting were significantly higher than those of Series N. The neutral axis ratios are also given in Table 1. Table 2 gives the various strengths and moduli of elasticity of Series A and Series N, measured at the time of the beam tests. The A-to-N ratios are also included in the table.

Table 1. Test results of beam specimens.

Specimen	M_c	M_{ct}	M_c/M_{ct}	M_y	M_{yt}	M_y/M_{yt}	M_u	M_{ut}	M_u/M_{ut}	η	F.P.
AS	3.61	1.72	2.10	7.55	7.38	1.02	9.14	7.98	1.15	0.524	flex.
NS	2.14	3.40	0.63	8.33	7.51	1.11	8.95	7.98	1.12	0.294	flex.
AS/NS	(1.69)			(0.91)			(1.02)			(1.78)	
AL	4.78	1.72	2.79	11.27	12.15	0.93	12.74	13.82	0.92	0.566	flex.
NL	2.38	3.40	0.70	12.05*12.45	-	-	12.05*13.82	-	-	0.350*	shear
AL/NL	(1.62)			(-)			(1.06)			(-)	

N.B.: moment in kN-m, η =neutral axis ratio at M_y , F.P.=failure pattern

Table 2. Mechanical properties of concrete.

Series	Strength (MPa)			Young's modulus (GPa)	
	Compression	Flexure	Tension	Static	Dynamic
A	40.3	3.18	2.69	17.8	20.9
N	40.6	6.29	3.01	24.9	28.0
A/N	0.99	0.50	0.90	0.72	0.74

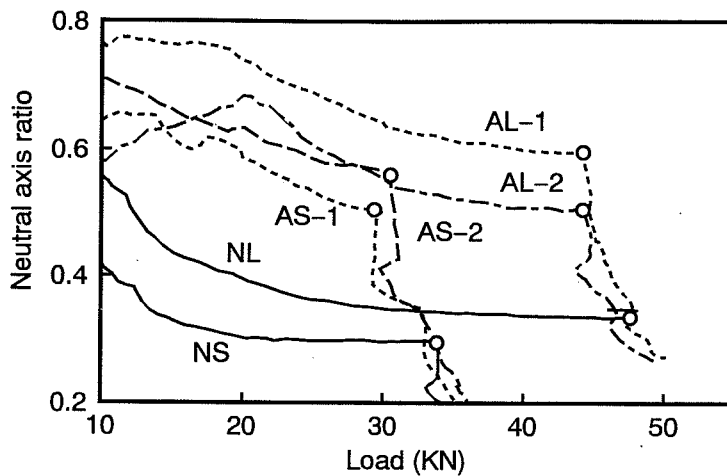


Fig. 4. Change of neutral axis ratio.

Discussions on test results

The calculated cracking bending moment (M_{ct}), yield starting bending moment (M_{yt}), and ultimate bending moment (M_{ut}) of the beams are given in *Table 1* in relation to the measured values. The values for Series A are averages of the two beams. The cracking moment, M_{ct} , was calculated by the elastic analysis of beams in which the extreme fiber stress was assumed to be the flexural strength of concrete, f_b . As for the yield starting moment, M_{yt} was calculated by assuming the strain distribution of concrete at the time of the yielding of the steel bars to be linear elastic. Here the ratio of measured Young's modulus of concrete to that of the bars (206 GPa) was adopted as the Young's modulus ratio. M_{ut} was calculated using a simple equation, which assumes the stress block of concrete to be rectangular, from the yield strength of the bars and compressive strength of concrete.

The measured M_c of the Series A beams is 2 to 3 times the calculated value in both cases. Such large differences are explained as follows: the cracking due to ASR reduced the strength of the standard test specimens, thus reducing the calculated M_{ct} values for Series A, while it increased the cracking load on the reinforced beam specimens in which the reinforcing bars restrain the ASR-induced expansion of concrete, causing chemical prestress. For this reason, the cracking bending moment cannot be related to the test results of the specimens for the strength test. As for Series N, the measured values are lower than the values calculated by assuming the extreme fiber stress to be f_b . This may be attributed to the effect of drying shrinkage as well as of the scale effect (Uchida *et al.* 1992).

Regarding the S beams, the measured M_y in Series A is close to the values calculated in consideration of E_c . For N beam, the measured one is approximately 10% higher than the calculation. Regarding the L beams, the measured values are slightly lower than the calculated value. Taking into account the fact that the apparent yield moment increases as the beam specimen size decreases (Koyanagi *et al.* 1989), M_y decreased in case of heavily deteriorated beams. In some instances of the past loading tests, no remarkable differences were found between the yield load of ASR-damaged beams and corresponding undamaged one. The reason may be that the cracking was not so severe and they did not cause such large reductions

in the neutral axis ratio as in the present testing.

In case of deteriorated beams, expansion due to ASR was arrested by reinforcing steel and the prestress was generated. During the loading test, the changing process of a neutral axis depth was measured. In case of ordinary reinforced concrete beams, the depth of neutral axis changed suddenly after cracking. In case of deteriorated beams, on the other hand, the change was small even after cracking and the presence of prestress was recognized.

After yield initiation of reinforcing steel for ASR-affected beams, the depth of neutral axis decreased rapidly because flexural cracks developed rapidly in cracking parts and the moment arm length increased. This leads to an increase in the resisting bending moment. The ultimate strengths of both series were therefore the same as in case of flexural failure.

ANALYSIS OF DEFORMATION

Method of analysis

Effects of the induced stresses caused by the restriction of ASR expansion on the bending moment at the yield starting point M_y and of load-deflection curve of the beam were examined analytically. The change of Young's modulus due to ASR was also examined. The object of the analysis was limited to S beam specimens which failed in flexure both in Series A and N.

The analysis was made in such a way that a certain amount of initial tensile pre-strain was given in reinforcing bars and corresponding prestress was in concrete. Moment-curvature relationships in a cross section were calculated with the "plane strain remaining" assumption and the stress equilibrium law. The stress-strain relationship of steel reinforcement was assumed to be elasto-plastic and that of concrete both in compression and in tension was to be linear elastic. Two kinds of Young's modulus were adopted; $E_c = 25$ and 18 GPa (see Table 2). Four levels of initial pre-strain were selected; i.e. 0, 500, 1200 and 1500×10^{-6} . The strain at yield point was 1850×10^{-6} as an average.

Result of analysis

The relationship between the yield starting moment to the initial strain in reinforcement and Young's modulus of concrete is illustrated in Fig. 5. M_y decreased when E_c was small, but the effect was not so remarkable. M_y decreased when the prestrain increased. But the effect of the pre-strain was so small as less than 10% when the initial strain was smaller than 60% of the yield point strain. The effect of the initial strain increased remarkably when it exceeded 80% of the yield strain, especially under smaller E_c .

Analytical load-deflection diagrams of the beam specimens under various initial strain are shown in Fig. 6. When the initial strain increased, the slope of the initial part of the diagram, i.e. the flexural rigidity, increased and the initial cracking load, which corresponded to the point where slope of the curve changed suddenly, also increased. This is because of the effect of the chemical prestress induced by the restriction of ASR expansion.

The change of the neutral axis ratio during loading is illustrated in Fig. 7. In Series N the neutral axis ratio dropped suddenly from ca. 0.5 to 0.3 at cracking. When the initial strain increased, the dropping point, i.e. the cracking load, increased, whereas the degree of dropping decreased. At the yield starting point, the neutral axis ratio increased as the initial pre-strain increased, and the yield load

decreased slightly, as mentioned before. After yield started in Series A, the neutral axis ratio decreased rapidly and load increased slightly because the moment arm length increased. Finally, the load in Series A coincided with that in Series N.

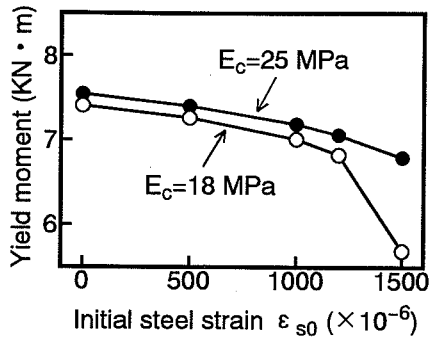


Fig. 5. Initial pre-strain vs. yield starting moment.

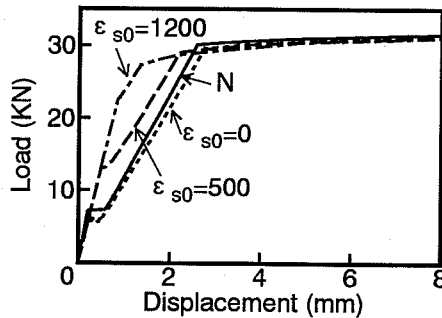


Fig. 6. Load-displacement diagram (analysis).

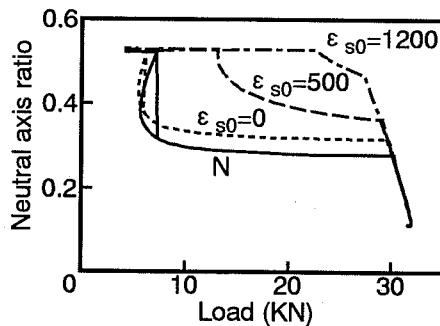


Fig. 7. Neutral axis ratio vs. load (analysis).

The reason why ASR increases the neutral axis ratio is discussed below. The property of a beam with severe cracks by ASR is considered to be shifted from that of reinforced concrete to prestressed concrete by the presence of induced

stresses. In other words, tensile force on the bars causes an axial compressive force in concrete, which increases the effective cross-section, lowering the neutral axis at the time of yield starting, and M_y corresponding to the yield starting point is reduced when compared with normal N beams. This is also affected by the reduction of Young's modulus. Since the reduction in E_c of concrete on the compression side may depend on the beam size, it is not clear if the E_c values agree with those determined from the standard test specimens.

CONCLUSIONS

Loading tests were conducted on singly reinforced concrete beams without shear reinforcement which were severely deteriorated with many wide cracks by ASR. Analytical study was also made. The following conclusions were obtained:

- (1) Severe ASR damage increases the neutral axis ratio at the time of yield starting when compared with undamaged beams. This reduces the arm length of the moment of the internal force, and consequently reduces the yield starting bending moment.
- (2) The increase in the neutral axis ratio is not only due to the apparent reduction of Young's modulus of concrete, but also due to the presence of prestress (prestrain) caused by the ASR-induced expansion restrained by the bars.
- (3) The reduction of yield starting moment is remarkable when the prestrain is quite large and the Young's modulus is low enough.
- (4) After the yield starting of bars, the deformation of the bars concentrates on the cracked portions. This reduces the neutral axis ratio rapidly and increases the arm length, and thus the ultimate load-bearing capacities in the case of flexural failure are independent of the damage of ASR.
- (5) Load-deflection relationships and change of neutral axis are well simulated by analysis, where the effect of the stress caused by the restriction of ASR expansion is taken into considerations.

REFERENCES

Cope, R.J. & Slade, L. 1992, 'Effect of AAR on shear capacity of beams, without shear reinforcement', Conference papers of 9th Int. Conf. on AAR, The concrete Society, 1, 184-191.

Hobbs, D.W. 1988, *Alkali-silica reaction in concrete*, Thomas Telford Ltd., London.

Inoue, S., Fujii, M., Kobayashi, K. & Nakano, K. 1989, 'Structural behaviors of reinforced concrete beams affected by alkali-silica reaction', Proc. 8th Int. Conf. on AAR, eds Okada, K., Nishibayashi, S. & Kawamura, M., Kyoto, Japan, 727-732.

Koyanagi, W., Rokugo, K. & Ishida, H. 1987, 'Failure behavior of reinforced concrete beams deteriorated by alkali-silica reactions', Proc. 7th Int. Conf. on AAR, ed. Grattan-Bellow, P.E., Ottawa, Canada, Noyes Publ., 141-145.

Koyanagi, W., Rokugo, K. & Iwase, H. 1989, 'Stress-strain relationship of reinforcing bars in concrete and mechanical behavior of RC beams in flexure', *Concrete Library of JSCE*, 12, 53-65.

Uchida, Y., Rokugo, K. & Koyanagi, W. 1992, 'Application of fracture mechanics to size effect on flexural strength of concrete', *Concrete Library of JSCE*, 20, 87-97.